

Signatures of Indistinguishability in Bosonic Many-Body Dynamics

Tobias Br unner,¹ Gabriel Dufour,^{1,2} Alberto Rodr iguez,¹ and Andreas Buchleitner^{1,*}

¹Physikalisches Institut, Albert-Ludwigs-Universit t-Freiburg, Hermann-Herder-Stra e 3, D-79104 Freiburg, Germany

²Freiburg Institute for Advanced Studies, Albert-Ludwigs-Universit t-Freiburg, Albertstra e 19, D-79104 Freiburg, Germany



(Received 19 October 2017; published 22 May 2018)

The dynamics of bosons in generic multimode systems, such as Bose-Hubbard models, are not only determined by interactions among the particles, but also by their mutual indistinguishability manifested in many-particle interference. We introduce a measure of indistinguishability for Fock states of bosons whose mutual distinguishability is controlled by an internal degree of freedom. We demonstrate how this measure emerges both in the noninteracting and interacting evolution of observables. In particular, we find an unambiguous relationship between our measure and the variance of single-particle observables in the noninteracting limit. A nonvanishing interaction leads to a hierarchy of interaction-induced interference processes, such that even the expectation value of single-particle observables is influenced by the degree of indistinguishability.

DOI: 10.1103/PhysRevLett.120.210401

Interference between indistinguishable particles is common to all many-particle quantum systems. Since the observation of the interference of two photons on a beam splitter by Hong, Ou, and Mandel (HOM) [1], the highly nontrivial character [2–7] of many-particle interference has been demonstrated in extensive studies of photons transmitted through multimode beam splitter arrangements [8–21]. While these studies are restricted to noninteracting particles, it is clear that interference also occurs in the presence of interactions. This was shown for HOM-type interference [22–26], in the dynamics of a bosonic Josephson junction [27,28], or in quantum walks [29–33]. However, these results are limited to two particles or two external modes, and a systematic understanding of the interplay between interactions and many-particle interference in the time evolution of general many-particle systems is still lacking. This fundamental question is, however, key to a variety of complex quantum phenomena, such as dynamical equilibration after a quench [34–36], correlation formation [37,38], or transport in interacting many-body systems [39,40]. Furthermore, certification of the bosonic and fermionic, as well as the (in)distinguishable character of particles [12,14,41–44], could also be achieved by identifying the corresponding interference fingerprints in the (interacting) dynamics.

Hence, it is the purpose of this work to systematically explore the impact of particles' indistinguishability on the time evolution of interacting many-body systems. We consider bosons that occupy a discrete set of coupled modes and whose mutual (in)distinguishability is controlled by an additional internal degree of freedom. First, we define a measure of the *degree of indistinguishability* (DOI) of many-body configurations, which is adapted to the study of interacting systems evolving continuously in

time from an arbitrary initial Fock state. This is in contrast to other DOI measures introduced in noninteracting photonic scattering setups [42,45–48]. We show that our measure has an intuitive interpretation in terms of two-particle interference. In the noninteracting case, it correlates directly with the *variance* of experimentally accessible single-particle observables (IPOs), as demonstrated in Fig. 1. Remarkably, in the presence of interactions, the DOI is also imprinted on the bare *expectation values* of IPOs.

Let us consider a general many-particle system with a discrete set of mutually coupled external modes $l \in \{1, 2, \dots, L\}$ (e.g., photonic input and output modes coupled via a beam splitter array, or tunnel-coupled sites

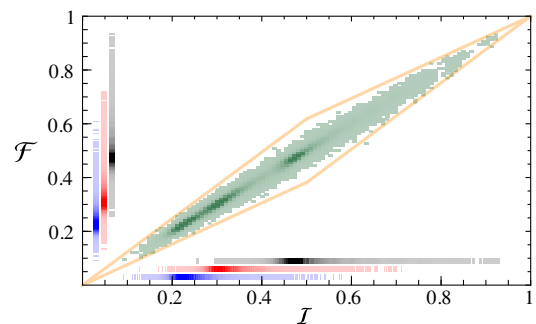


FIG. 1. Density histogram of the normalized time-averaged variance \mathcal{F} [Eq. (4)] of the on-site atomic density (at an arbitrary site) versus the DOI measure \mathcal{I} [Eq. (1)] of the initial Fock state in a noninteracting Bose-Hubbard system. We consider a total of 3×10^5 initial states sampled uniformly over the available Hilbert space of a system with $L = 12$ sites and $N = 24$ bosons of $S = 2$ (black), 3 (red), and 4 (blue) distinct species. Projections of the histogram along the axes are shown independently for each S . Thick solid lines indicate our bound (5) on the \mathcal{F} - \mathcal{I} correlation.

in an optical lattice), and with a discrete set of internal states, or “species,” $\sigma \in \{\sigma_1, \sigma_2, \dots, \sigma_S\}$ (e.g., photon polarization or hyperfine states of atoms). For a many-body Fock state $|\Psi\rangle = \otimes_{l,\sigma} |N_{l,\sigma}\rangle$, with $N_{l,\sigma}$ bosons of species σ in mode l , we propose the following quantitative measure of the DOI:

$$\mathcal{I} := \frac{\sum_{\sigma} \sum_{m \neq n} N_{m,\sigma} N_{n,\sigma}}{\sum_{m \neq n} N_m N_n}. \quad (1)$$

Here, $N_l := \sum_{\sigma} N_{l,\sigma}$ denotes the total number of particles in mode l , such that $\mathcal{I} \in [0, 1]$. This measure takes the value 1 only when all particles are indistinguishable (i.e., only one species is present). When each particle is of a different species (maximally distinguishable), then, consistently, $\mathcal{I} = 0$. However, this minimum value is also reached when all particles of a given species occupy the same mode. According to our measure, the DOI does not solely depend on the repartition of particles among species, but also on how the species are distributed over the external modes [49]. This interplay between external and internal degrees of freedom, although discussed for the indistinguishability of two photons [50,51], has not been clearly resolved in previously introduced DOI measures [42,45–48].

In the following, we demonstrate how this measure emerges in the dynamics of interacting and noninteracting systems. In order to assess the consequences of (in)distinguishability in the evolution, we require both the Hamiltonian and the measured observables to be *species-blind*: they neither resolve, nor modify, the internal degree of freedom σ of the particles [52]. In particular, the number of bosons per species is conserved.

We first consider the *noninteracting case*, where the Hamiltonian takes the general form of a species-blind IPO, $\mathcal{H}_0 = \sum_{i,j,\sigma} J_{ij} a_{i,\sigma}^{\dagger} a_{j,\sigma}$, and the time-evolution of the bosonic operators is given by the matrix elements $c_{lm}(t)$ of the single-particle unitary evolution operator: $a_{l,\sigma}(t) = \sum_m c_{lm}(t) a_{m,\sigma}$. Under these conditions, many-particle interference is known to manifest itself only on the level of two-particle or higher-order observables [53]. Indeed, the expectation value of a general species-blind two-particle observable (2PO), $\mathcal{O}_2 = \sum_{i,j,k,l,\sigma,\rho} O_{ijkl} a_{i,\sigma}^{\dagger} a_{j,\rho}^{\dagger} a_{k,\sigma} a_{l,\rho}$, in a Fock state $|\Psi\rangle$ reads

$$\begin{aligned} \langle \mathcal{O}_2(t) \rangle_{\Psi} &= \sum_{i,j,k,l} O_{ijkl} \left(\sum_{m,n} C_{ijkl}^{mn}(t) N_m (N_n - \delta_{mn}) \right. \\ &\quad \left. + \sum_{m \neq n, \sigma} C_{jikl}^{mn}(t) N_{m,\sigma} N_{n,\sigma} \right). \end{aligned} \quad (2)$$

The above expression can be interpreted as a sum over two-particle paths consisting of forward time evolution from the initial state, application of the observable and backward time evolution back to the same state [52]. The first line of Eq. (2) collects contributions of “ladder” paths, where the two particles initially in modes m and n return to their

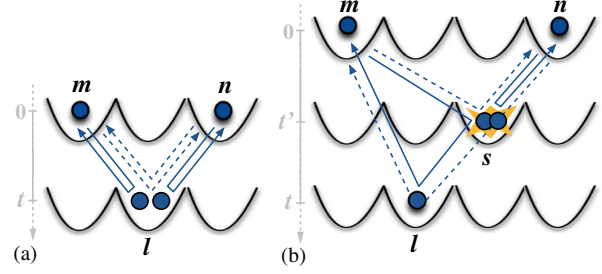


FIG. 2. Two-particle paths of indistinguishable bosons: ladder (solid lines) and crossed (dashed lines). (a) Noninteracting: Processes $(m, n) \rightleftharpoons (l)$ associated with the amplitude $C_{lll}^{mn}(t)$ in Eq. (3) contribute to the variance $\Delta \mathcal{N}_l(t)$ of the total density operator \mathcal{N}_l of the l th mode. (b) Interacting: Processes with amplitude $D_{ll}^{mn}(t)$ in Eq. (7) (which accounts for the interaction on all modes s , at times $t' \leq t$, before one of the particles visits mode l) contribute to the expectation value $\langle \mathcal{N}_l(t, U) \rangle$.

respective starting positions. These are associated with an amplitude $C_{lll}^{mn}(t) := c_{im}^*(t) c_{jn}^*(t) c_{km}(t) c_{ln}(t)$ and a multiplicity $N_m N_n$. They are common to all many-body configurations with the same initial total density distribution. Hence, they bear no information on the (in)distinguishability of the bosons. The second line in Eq. (2) represents additional “crossed” paths, where two particles of the same species σ , initially in modes m and n , are swapped, arriving in modes n and m , respectively. Such processes have species- (i.e., σ -) dependent multiplicities $N_{m,\sigma} N_{n,\sigma}$, and therefore, they bear information on the (in)distinguishability of the initially prepared many-particle configuration. Figure 2(a) illustrates these ladder and crossed two-body processes for an observable that is local in the mode index.

The multiplicities of the crossed and ladder paths appear respectively in the numerator and denominator of our DOI measure [Eq. (1)], which therefore weighs the relative importance of the two types of processes in the expectation value of any 2PO [Eq. (2)]. We find that our measure manifests itself most directly when the 2PO under consideration is the square of a species-blind IPO, $\mathcal{O}_1 = \sum_{i,j,\sigma} O_{ij} a_{i,\sigma}^{\dagger} a_{j,\sigma}$, as this ensures that the factors $N_{m,\sigma} N_{n,\sigma}$ appear dressed by real and positive coefficients in Eq. (2). In particular, we consider the variance $\Delta \mathcal{O}_1(t) = \langle \mathcal{O}_1^2(t) \rangle_{\Psi} - \langle \mathcal{O}_1(t) \rangle_{\Psi}^2$ of on-site density operators \mathcal{N}_l ,

$$\Delta \mathcal{N}_l(t) = \sum_{m \neq n, \sigma} C_{lll}^{mn}(t) N_{m,\sigma} (N_{n,\sigma} + 1), \quad (3)$$

with amplitudes $C_{lll}^{mn}(t) = |c_{lm}(t) c_{ln}(t)|^2$. By averaging over time and subtracting the σ -independent contribution in Eq. (3), the normalized time-averaged variance of the IPO in the Fock state $|\Psi\rangle$ reads

$$\mathcal{F} := \frac{\overline{\Delta \mathcal{N}_l(t)} - \Delta_0}{\Delta_1 - \Delta_0} = \frac{\sum_{\sigma} \sum_{m \neq n} \overline{C_{lll}^{mn}(t)} N_{m,\sigma} N_{n,\sigma}}{\sum_{m \neq n} \overline{C_{lll}^{mn}(t)} N_m N_n}, \quad (4)$$

where the overbar denotes time average, and $\Delta_{0,1}$ correspond to $\overline{\Delta N_1(t)}$ in a state with the same total density distribution as $|\Psi\rangle$ but with $\mathcal{I} = 0$ (Δ_0) or $\mathcal{I} = 1$ (Δ_1) (i.e., in a fully distinguishable configuration, or in the state involving only one species, respectively [54]). A comparison of Eqs. (1) and (4) shows that, for a narrow distribution of the $C_{lll}^m(t)$ over $m \neq n$, the measurement of \mathcal{F} directly gives access to the DOI. Specifically, we find that [52]

$$|\mathcal{F} - \mathcal{I}| \lesssim \frac{W_C}{\mu_C} \min(\mathcal{I}, 1 - \mathcal{I}), \quad (5)$$

where W_C and μ_C are, respectively, the standard deviation and the mean of the $C_{lll}^m(t)$ for all pairs $m \neq n$.

It is instructive to study the behavior of our DOI measure in the special case of a two-mode system, such as a multicomponent, species-blind, noninteracting Bose-Hubbard Hamiltonian (BHH) [52] with $L = 2$ sites. In any two-mode system, only one coefficient, $C_{lll}^{12}(t)$, contributes to \mathcal{F} , which therefore reproduces *exactly* the DOI measure \mathcal{I} . For two bosonic species $\sigma \in \{\uparrow, \downarrow\}$, and fixed total particle number N , the configuration space of the system is determined by three parameters: the mode population imbalance, $M = N_1 - N_2$, and the species imbalances per site, $\delta_1 = N_{1,\uparrow} - N_{1,\downarrow}$ and $\delta_2 = N_{2,\uparrow} - N_{2,\downarrow}$. The DOI measure then reads

$$\mathcal{I} = \frac{1}{2} + \frac{2\delta_1\delta_2}{N^2 - M^2}. \quad (6)$$

For $M = 0$, the space of nonequivalent Fock configurations is spanned by $\delta_1 \in [0, N/2]$ and $|\delta_2| \leq \delta_1$, and it is charted in Fig. 3 for $N = 8$. According to Eq. (6), having all particles of the same species [$\delta_1 = \delta_2 = N/2$] corresponds to $\mathcal{I} = 1$, whereas complete spatial separation of the two species [$\delta_1 = -\delta_2 = N/2$] implies $\mathcal{I} = 0$. As shown in the top inset of Fig. 3, these two initial states seed, respectively, maximum and minimum values of the density fluctuation $\Delta N_1(t)$, as a direct consequence of the presence or absence of the two-particle crossed terms in Eq. (2) and Fig. 2(a). Furthermore, all states with $\delta_2 = 0$ —although having different species imbalance $\delta_1 + \delta_2$ —have the same $\mathcal{I} = 1/2$ and yield the same fluctuation of IPOs over time if the bosons do not interact. Conversely, states with equal species imbalances can exhibit different DOI values and hence dissimilar fluctuations.

Let us proceed to larger numbers of modes and species. We numerically demonstrate a remarkable \mathcal{F} - \mathcal{I} correlation in a species-blind BHH with $L = 12$ sites and a total of $N = 24$ noninteracting bosons, as shown in Fig. 1. We sample uniformly 10^5 initial states out of the total available Fock space for each of the cases of $S = 2, 3$, and 4 distinct species. For each state, \mathcal{F} is calculated using Eq. (4) and plotted versus the DOI value \mathcal{I} , together with the bound provided by Eq. (5). We observe that the \mathcal{F} - \mathcal{I} correlation becomes even more pronounced for larger L and/or N [55]. These results demonstrate that our DOI measure is at the

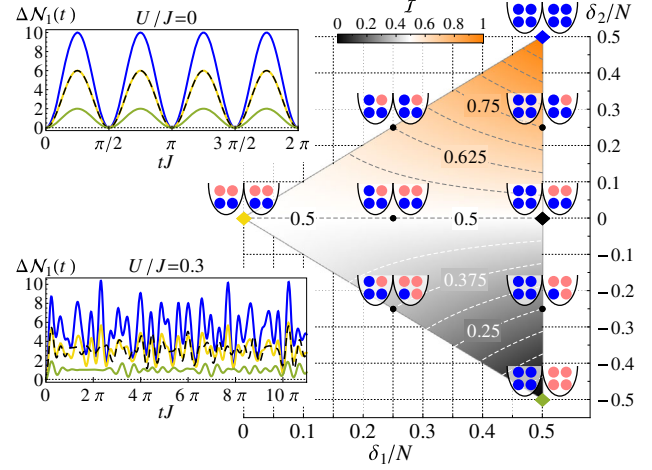


FIG. 3. Density plot of the DOI for a two-species (blue/red) double well in the δ_1 - δ_2 plane for $M = 0$ [see Eq. (6)], including all nine nonequivalent configurations for $N = 8$. Top and bottom insets show $\Delta N_1(t)$ for four initial Fock configurations [$\mathcal{I} = 1$ (blue, totally indistinguishable), 0.5 (yellow, black dashed), and 0 (green, maximally distinguishable)] for the noninteracting and interacting ($U/J = 0.3$) cases, respectively.

core of the time evolution of 2POs in noninteracting systems [see Eq. (2)], and furthermore, that it can be characterized from the *variance* of IPOs such as the on-site density of cold bosons in optical lattices.

We now expand our analysis to the *interacting case*, where, remarkably, the DOI is revealed already in the *expectation value* of IPOs. To see this, we complement the Hamiltonian by a species-blind, two-body interaction term $\mathcal{V} = \sum_{i,j,k,l,\sigma,\rho} V_{ijkl} a_{i,\sigma}^\dagger a_{j,\rho}^\dagger a_{k,\sigma} a_{l,\rho}$. For simplicity, we elaborate on the case of contact “on-mode” interactions, $V_{ijkl} = (U/2)\delta_{ij}\delta_{jk}\delta_{kl}$; our subsequent results, however, are valid for the most general \mathcal{V} [52]. In contrast to the noninteracting scenario, $a_{l,\sigma}(t)$ is now nonlinear in the initial creation and annihilation operators. Hence, in the Heisenberg picture, any IPO develops, over time, a hierarchy of contributions in the form of two- and many-particle observables whose importance is weighted by the interaction strength. A perturbative treatment shows $\mathcal{O}_1(t, U) = \mathcal{O}_1(t, 0) + (Ut)\mathcal{P}(t) + \mathcal{O}[(Ut)^2]$ [52]. Here, $\mathcal{O}_1(t, 0)$ is a IPO corresponding to the noninteracting evolution, with an expectation value independent of the particles’ (in)distinguishability. In contrast, $\mathcal{P}(t)$ is a 2PO with time-dependent matrix elements, and its expectation value reads

$$\langle \mathcal{P}(t) \rangle_\Psi = 2\Im \sum_{i,j} O_{ij} \left(\sum_{m,n} D_{ij}^{mn}(t) N_m (N_n - \delta_{mn}) + \sum_{m \neq n, \sigma} D_{ij}^{m\sigma}(t) N_{m,\sigma} N_{n,\sigma} \right), \quad (7)$$

where $D_{ij}^{mn}(t)$ is the amplitude of the ladder and crossed two-particle paths arising due to the interaction [52]. These

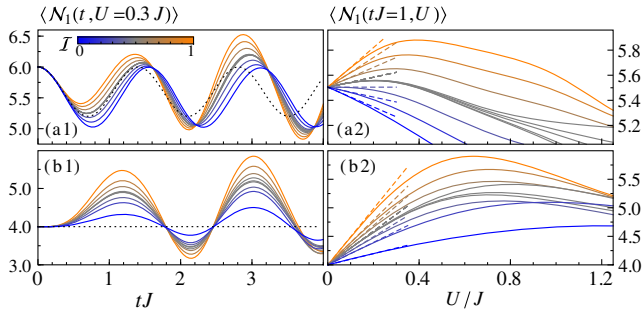


FIG. 4. Expectation value $\langle \mathcal{N}_1(t, U) \rangle$ in the two-species double well with a tilt $F\mathcal{N}_2$, for $N = 8$ and (a) $M = 4, F = 4J$, (b) $M = 0, F = 3J$, for all nonequivalent Fock states (color determined by the DOI value \mathcal{I} as indicated). The left (right) column shows the evolution versus t (U) for fixed $U/J = 0.3$ ($tJ = 1$). Solid lines are numerical results, while dashed lines show the prediction of first order perturbation theory. Dotted lines in the left panels indicate the case $U = 0$.

are illustrated in Fig. 2(b) for the one-mode density \mathcal{N}_1 as IPO.

By analogy with the result for 2POs in the noninteracting case [compare the structure of (7) to that of (2)], the DOI measure \mathcal{I} can be identified in the expectation value of IPOs in the interacting case, dressed by the amplitudes $D_{ij}^{mn}(t)$. Interactions therefore imprint the DOI on the bare expectation value of IPOs. This is demonstrated in Fig. 4, where we show the expectation value $\langle \mathcal{N}_1(t, U) \rangle$ for the two-species two-site BHH [27,28,56–63] subject to a tilt (to ensure a nonvanishing Ut correction [64]). Within a regime of small Ut , which depends on the system under consideration, the evolution of the on-site density is well described by Eq. (7). In particular, the initial slopes of the curves in Figs. 4(a2) and (b2) are uniquely determined by \mathcal{I} . For larger interaction strengths and/or times, higher-order terms contribute to the expectation value of the observable, which additionally probe three-particle and higher processes [causing, e.g., states with the same $\mathcal{I} = 0.5$ to exhibit independent trajectories—see panels (a2) and (b2) of Fig. 4]. Nonetheless, the correlation between $\langle \mathcal{N}_1(t, U) \rangle$ and \mathcal{I} persists beyond first order perturbation. This suggests that our measure of the DOI based on two-particle paths remains meaningful even in the presence of higher-order processes.

Indeed, also the long-time signals $\Delta \mathcal{N}_1(t, U \neq 0)$, although more involved than in the noninteracting case due to the appearance of extra frequencies (compare the top and bottom insets of Fig. 3), indicate that the time-averaged density fluctuation still correlates with the DOI of the initial state. This is demonstrated in Fig. 5, where we show $\Delta \mathcal{N}_1(t, U)$ as a function of U [52]. For states with a homogeneous initial distribution of particles (first row of Fig. 5), one observes a striking correlation between $\Delta \mathcal{N}_1(t, U)$ and \mathcal{I} over the entire range of interaction strengths (also for $L > 3$ —not shown in the figure). For

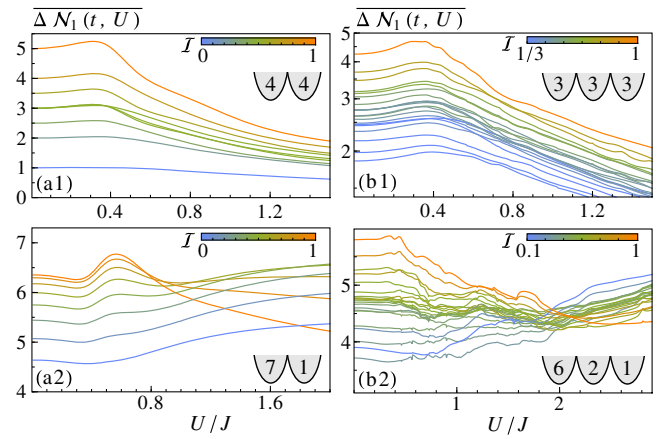


FIG. 5. Time-averaged density fluctuation $\overline{\Delta \mathcal{N}_1(t, U)}$ versus interaction strength $U/J > 0$, for a BHH with two bosonic species: (a) $L = 2, N = 8$ and (b) $L = 3, N = 9$, for the symbolically indicated initial densities and all nonequivalent Fock states (color determined by the DOI value \mathcal{I} as indicated). Note the vertical log scale in (b1).

states with a strongly imbalanced initial distribution of particles (second row of Fig. 5), this correlation also holds for weak interactions, but is lost for larger values of U . Closer inspection of the system’s spectral structure shows that, in the regime of strong interactions, the dynamics are dominated by Fock states with the same interaction energy as the initial state, which, in the imbalanced case, include states with dissimilar density distributions [e.g., $\{7, 1\}$ and $\{1, 7\}$ in the double well]. The interaction-mediated higher-order processes connecting these states then contribute predominantly to $\Delta \mathcal{N}_1(t, U)$, breaking the correlation to the DOI measure \mathcal{I} . A detailed characterization of this effect will be the subject of future work.

We conclude by generalizing our DOI measure to superpositions of Fock states $|\Psi\rangle = \sum_j c_j |\psi_j\rangle$, where each term has the same total density distribution but a different number of particles per species. The expectation value of a species-blind observable in such a state is additive, since by definition, the observable cannot change the number of particles per species. Thus, we can additively generalize our DOI measure as $\mathcal{I}_\Psi = \sum_j |c_j|^2 \mathcal{I}_{\psi_j}$. For the exemplary Hong-Ou-Mandel state $|\Psi\rangle = (\sqrt{\alpha} a_{1,\uparrow}^\dagger a_{2,\uparrow}^\dagger + \sqrt{1-\alpha} a_{1,\uparrow}^\dagger a_{2,\downarrow}^\dagger) |\text{vac}\rangle$, our measure \mathcal{I} coincides with Mandel’s indistinguishability parameter α [67]. Using the additivity property of \mathcal{I} , the effects of indistinguishability in various generalizations of the Hong-Ou-Mandel setup (e.g., nonmonotonicity in four-photon interference [2,3]) are embedded in a more general framework.

We have introduced a measure of the degree of indistinguishability (DOI) of a many-particle quantum state, which is derived from the structure of two-particle transition amplitudes, and could be accessed in experiments by monitoring the fluctuations of one-particle observables.

Our measure incorporates the significance of internal as well as of external degrees of freedom for the DOI and for the associated many-particle interferences, and it notably exploits the information encoded in the continuous dynamical many-particle evolution—inaccessible in many-particle scattering scenarios. Our analysis also shows that *interaction-induced* interference reveals the DOI already in the *expectation value* of single-particle observables, and that the DOI remains a meaningful concept in the presence of interactions. The characteristic dynamical features observed here must have a structural counterpart in the underlying energy spectra and many-particle eigenstates, which deserve further investigation. We emphasize that our formalism and conclusions apply to general many-particle scenarios beyond the Bose-Hubbard model chosen to illustrate our results numerically.

T. B. expresses gratitude to the German Research Foundation (IRTG 2079) for financial support and thanks Mattia Walschaers and Florian Meinert for helpful discussions. G. D. and A. B. acknowledge support by the EU Collaborative project QuProCS (Grant Agreement No. 641277). Furthermore, G. D. is thankful to the Alexander von Humboldt foundation. The authors acknowledge support by the state of Baden-Württemberg through bwHPC and the German Research Foundation (DFG) through Grant No. INST 40/467-1 FUGG.

* a.buchleitner@physik.uni-freiburg.de

- [1] C. K. Hong, Z. Y. Ou, and L. Mandel, *Phys. Rev. Lett.* **59**, 2044 (1987).
- [2] M. C. Tichy, H.-T. Lim, Y.-S. Ra, F. Mintert, Y.-H. Kim, and A. Buchleitner, *Phys. Rev. A* **83**, 062111 (2011).
- [3] Y.-S. Ra, M. C. Tichy, H.-T. Lim, O. Kwon, F. Mintert, A. Buchleitner, and Y.-H. Kim, *Proc. Natl. Acad. Sci. U.S.A.* **110**, 1227 (2013).
- [4] S. H. Tan, Y. Y. Gao, H. de Guise, and B. C. Sanders, *Phys. Rev. Lett.* **110**, 113603 (2013).
- [5] N. Spagnolo, C. Vitelli, L. Aparo, P. Mataloni, F. Sciarrino, A. Crespi, R. Ramponi, and R. Osellame, *Nat. Commun.* **4**, 1606 (2013).
- [6] S. Agne, J. Jin, J. Z. Salvail, K. J. Resch, T. Kauten, E. Meyer-Scott, D. R. Hamel, G. Weihs, and T. Jennewein, *Phys. Rev. Lett.* **118**, 153602 (2017).
- [7] A. J. Menssen, A. E. Jones, B. J. Metcalf, M. C. Tichy, S. Barz, W. S. Kolthammer, and I. A. Walmsley, *Phys. Rev. Lett.* **118**, 153603 (2017).
- [8] M. C. Tichy, M. Tiersch, F. Mintert, and A. Buchleitner, *New J. Phys.* **14**, 093015 (2012).
- [9] S. Aaronson and A. Arkhipov, *Theory Comput.* **9**, 143 (2013).
- [10] M. Tillmann, S. H. Tan, S. E. Stoeckl, B. C. Sanders, H. de Guise, R. Heilmann, S. Nolte, A. Szameit, and P. Walther, *Phys. Rev. X* **5**, 041015 (2015).
- [11] V. Tamma and S. Laibacher, *Quantum Inf. Process.* **15**, 1241 (2016).
- [12] V. S. Shchesnovich, *Phys. Rev. Lett.* **116**, 123601 (2016).
- [13] J.-D. Urbina, J. Kuipers, S. Matsumoto, Q. Hummel, and K. Richter, *Phys. Rev. Lett.* **116**, 100401 (2016).
- [14] M. Walschaers, J. Kuipers, J. D. Urbina, K. Mayer, M. C. Tichy, K. Richter, and A. Buchleitner, *New J. Phys.* **18**, 032001 (2016).
- [15] A. Crespi, R. Osellame, R. Ramponi, D. J. Brod, E. F. Galvão, N. Spagnolo, C. Vitelli, E. Maiorino, P. Mataloni, and F. Sciarrino, *Nat. Photonics* **7**, 545 (2013).
- [16] M. A. Broome, A. Fedrizzi, S. Rahimi-Keshari, J. Dove, S. Aaronson, T. C. Ralph, and A. G. White, *Science* **339**, 794 (2013).
- [17] J. B. Spring, B. J. Metcalf, P. C. Humphreys, W. S. Kolthammer, X.-M. Jin, M. Barbieri, A. Datta, N. Thomas-Peter, N. K. Langford, D. Kundys, J. C. Gates, B. J. Smith, P. G. R. Smith, and I. A. Walmsley, *Science* **339**, 798 (2013).
- [18] M. Tillmann, B. Dakić, R. Heilmann, S. Nolte, A. Szameit, and P. Walther, *Nat. Photonics* **7**, 540 (2013).
- [19] J. Carolan, J. D. A. Meinecke, P. J. Shadbolt, N. J. Russell, N. Ismail, K. Wörhoff, T. Rudolph, M. G. Thompson, J. L. O'Brien, J. C. F. Matthews, and A. Laing, *Nat. Photonics* **8**, 621 (2014).
- [20] L. Latmiral, N. Spagnolo, and F. Sciarrino, *New J. Phys.* **18**, 113008 (2016).
- [21] H. Wang, Y. He, Y.-H. Li, Z.-E. Su, B. Li, H.-L. Huang, X. Ding, M.-C. Chen, C. Liu, J. Qin *et al.*, *Nat. Photonics* **11**, 361 (2017).
- [22] E. Andersson, M. T. Fontenelle, and S. Stenholm, *Phys. Rev. A* **59**, 3841 (1999).
- [23] A. M. Kaufman, B. J. Lester, C. M. Reynolds, M. L. Wall, M. Foss-Feig, K. R. A. Hazzard, A. M. Rey, and C. Regal, *Science* **345**, 306 (2014).
- [24] W. J. Mullin and F. Laloë, *Phys. Rev. A* **91**, 053629 (2015).
- [25] B. Gertjerenken and P. G. Kevrekidis, *Phys. Lett. A* **379**, 1737 (2015).
- [26] A. M. Kaufman, M. C. Tichy, F. Mintert, A. M. Rey, and C. A. Regal, [arXiv:1801.04670](https://arxiv.org/abs/1801.04670).
- [27] M. C. Tichy, J. F. Sherson, and K. Mølmer, *Phys. Rev. A* **86**, 063630 (2012).
- [28] G. Dufour, T. Brünner, C. Dittel, G. Weihs, R. Keil, and A. Buchleitner, *New J. Phys.* **19**, 125015 (2017).
- [29] Y. Lahini, M. Verbin, S. D. Huber, Y. Bromberg, R. Pugatch, and Y. Silberberg, *Phys. Rev. A* **86**, 011603 (2012).
- [30] X. Qin, Y. Ke, X. Guan, Z. Li, N. Andrei, and C. Lee, *Phys. Rev. A* **90**, 062301 (2014).
- [31] L. Wang, L. Wang, and Y. Zhang, *Phys. Rev. A* **90**, 063618 (2014).
- [32] P. M. Preiss, R. Ma, M. E. Tai, A. Lukin, M. Rispoli, P. Zupancic, Y. Lahini, R. Islam, and M. Greiner, *Science* **347**, 1229 (2015).
- [33] Q. Wang and Z.-J. Li, *Ann. Phys. (Amsterdam)* **373**, 1 (2016).
- [34] A. Polkovnikov, K. Sengupta, A. Silva, and M. Vengalattore, *Rev. Mod. Phys.* **83**, 863 (2011).
- [35] J. Eisert, M. Friesdorf, and C. Gogolin, *Nat. Phys.* **11**, 124 (2015).
- [36] A. M. Kaufman, M. E. Tai, A. Lukin, M. Rispoli, R. Schittko, P. M. Preiss, and M. Greiner, *Science* **353**, 794 (2016).
- [37] A. J. Daley, H. Pichler, J. Schachenmayer, and P. Zoller, *Phys. Rev. Lett.* **109**, 020505 (2012).

- [38] R. Islam, R. Ma, P. M. Preiss, M. E. Tai, A. Lukin, M. Rispoli, and M. Greiner, *Nature (London)* **528**, 77 (2015).
- [39] F. Meinert, M. J. Mark, E. Kirilov, K. Lauber, P. Weinmann, M. Gröbner, and H.-C. Nägerl, *Phys. Rev. Lett.* **112**, 193003 (2014).
- [40] R. Labouvie, B. Santra, S. Heun, S. Wimberger, and H. Ott, *Phys. Rev. Lett.* **115**, 050601 (2015).
- [41] C. F. Roos and A. Alberti and D. Meschede and P. Hauke, and H. Häffner, *Phys. Rev. Lett.* **119**, 160401 (2017).
- [42] M. Walschaers, J. Kuipers, and A. Buchleitner, *Phys. Rev. A* **94**, 020104 (2016).
- [43] N. Spagnolo, C. Vitelli, M. Bentivegna, D. J. Brod, A. Crespi, F. Flamini, S. Giacomini, G. Milani, R. Ramponi, P. Mataloni, R. Osellame, E. F. Galvão, and F. Sciarrino, *Nat. Photonics* **8**, 615 (2014).
- [44] T. Giordani, F. Flamini, M. Pompili, N. Viggianiello, N. Spagnolo, A. Crespi, R. Osellame, N. Wiebe, M. Walschaers, A. Buchleitner, and F. Sciarrino, *Nat. Photonics* **12**, 173 (2018).
- [45] H. de Guise, S.-H. Tan, I. P. Poulin, and B. C. Sanders, *Phys. Rev. A* **89**, 063819 (2014).
- [46] V. S. Shchesnovich, *Phys. Rev. A* **89**, 022333 (2014).
- [47] V. S. Shchesnovich, *Phys. Rev. A* **91**, 013844 (2015).
- [48] M. C. Tichy, *Phys. Rev. A* **91**, 022316 (2015).
- [49] We note that \mathcal{I} [Eq. (1)] can be written in terms of the inverse participation ratios (with respect to the external modes) of the density distributions, $\text{IPR}_\sigma = \sum_m N_{m,\sigma}^2 / N_\sigma^2$, where N_σ is the total number of σ -particles, and $\text{IPR} = \sum_m N_m^2 / N^2$. The DOI reads $\mathcal{I} = \sum_\sigma (N_\sigma^2 / N^2) (1 - \text{IPR}_\sigma) / (1 - \text{IPR})$ and can thus be directly related to the degree of localization of each species over the external modes (occupation of one mode $\Rightarrow \text{IPR}_\sigma = 1$, homogeneous spreading $\Rightarrow \text{IPR}_\sigma = L^{-1}$).
- [50] M. Tichy, F. de Melo, M. Kuś, F. Mintert, and A. Buchleitner, *Fortschr. Phys.* **61**, 225 (2013).
- [51] P. S. Turner, [arXiv:1608.05720](https://arxiv.org/abs/1608.05720).
- [52] See Supplemental Material at <http://link.aps.org/supplemental/10.1103/PhysRevLett.120.210401> for further details.
- [53] K. Mayer, M. C. Tichy, F. Mintert, T. Konrad, and A. Buchleitner, *Phys. Rev. A* **83**, 062307 (2011).
- [54] In an experimental estimation of \mathcal{F} , the quantity Δ_0 could be calculated theoretically if the parameters of the experimental Hamiltonian are known, without the need to engineer a state with $\mathcal{I} = 0$. The normalization factor, $\Delta_1 - \Delta_0$, can be ignored if one compares ratios of \mathcal{F} to ratios of \mathcal{I} .
- [55] As N increases, the percentage of Fock configurations which could potentially violate the bound of Eq. (5) decreases, while larger L reduces the ratio W_C / μ_C (see Supplemental Material).
- [56] H. T. Ng, C. K. Law, and P. T. Leung, *Phys. Rev. A* **68**, 013604 (2003).
- [57] X. Q. Xu, L. H. Lu, and Y. Q. Li, *Phys. Rev. A* **78**, 043609 (2008).
- [58] B. Juliá-Díaz, M. Guilleumas, M. Lewenstein, A. Polls, and A. Sanpera, *Phys. Rev. A* **80**, 023616 (2009).
- [59] B. Sun and M. S. Pindzola, *Phys. Rev. A* **80**, 033616 (2009).
- [60] R. Citro, A. Nadeo, and E. Orignac, *J. Phys. B* **44**, 115306 (2011).
- [61] L.-H. Lu, X.-Q. Xu, and Y.-Q. Li, *J. Phys. B* **44**, 145301 (2011).
- [62] P. Ziń, B. Oleś, and K. Sacha, *Phys. Rev. A* **84**, 033614 (2011).
- [63] P. Mujal, B. Juliá-Díaz, and A. Polls, *Phys. Rev. A* **93**, 043619 (2016).
- [64] The first order correction in Ut of $\mathcal{O}_1(t, U)$ vanishes if the IPO time evolution exhibits $U \rightarrow -U$ symmetry. This holds for certain IPOs in systems with a real Hamiltonian (preserved time-reversal symmetry) for which the noninteracting terms have bipartite symmetry (see Supplemental Material and Ref. [65,66]).
- [65] R. Mosseri, *J. Phys. A* **33**, L319 (2000).
- [66] U. Schneider, L. Hackermüller, J. P. Ronzheimer, S. Will, S. Braun, T. Best, I. Bloch, E. Demler, S. Mandt, D. Rasch, and A. Rosch, *Nat. Phys.* **8**, 213 (2012).
- [67] L. Mandel, *Opt. Lett.* **16**, 1882 (1991).